Middle-East Journal of Scientific Research 22 (4): 561-574, 2014
ISSN 1990-9233

DOI: 10.5829/idosi.mejsr.2014.22.04.874

Economic and Environmental Modeling of a MGT-SOFC Hybrid Combined Heat and Power System for Ship Applications

[1,2]M.Y. Abdollahzadeh Jamalabadi, [3]Payam Hooshmand and [4]Behnam Broumand

[1]Maritime University of Chabahar, Chabahar, Iran
[2]Graduate School of Mechanical and Aerospace Engineering, Gyeongsang National University, Jinju, South Korea
[3]Young Researchers and Elite Club, Mahabad Branch, Islamic Azad University, Mahabad, Iran
[4]Sharif University of Technology, Department of Mechanical Engineering, International Campus, Kish, Iran

Abstract: In this article, economic and environmental analysis of a combined heat and power system (CHP) system using solid oxide fuel cell (SOFC) - micro gas turbine (MGT) is investigated. Comprehensive electrochemical, thermal and exergetic calculations in the system are performed in order to get hold of accurate that is validated using available data in literature. A parameter study is accomplished based on the working pressure , rate of air flow into the system, fuel cell current density, fuel unit cost , capital cost ,and electricity price to evaluating the total cost rate including investment, operational and environmental are investigated. Results show that increasing of the working pressure and rate of air flow into the system; cause the economic performance of the system to reduce and the environmental emission to increase. Furthermore, the electrical energy cost is obtained 0.09 $\$kW^{-1}h^{-1}$ and payback period of the investment is about 5.4 years.

Key words: Mini gas turbine · Solid oxide fuel cell · Combined heat and power system · economic analysis · Environmental analysis · Energy system planning

INTRODUCTION

The world's increasing population, their energy demand, energy cost of exploration and production and the reduction of fossil fuel resources in recent decades have involved much studies in the field of emission-less and high monetary efficiency energy systems. So long as oil is used as a main source of energy, the cost of getting well a barrel of oil becomes greater than the energy content of it; production will stop no matter what the financial worth may be. Still majorly of alternative energy sources relying on fossil fuels, fuel cells are considered as a new tools in energy production which promising the diminution of environmental emissions because of using the electric potential in the chemical reaction of fuel to produce the electricity. Among the fuel cell systems the solid oxide fuel cell (SOFC) has paid more attention due to proper efficiency and consecutively generation of electricity and heat [1]. The ability of SOFC in being combined with diverse power systems and various types of gas turbines [2], low environmental pollution, suitable power density, independent power system from moving parts and low acoustic noise can play a chief role in the future power plant [3]. The hybrid systems the first time were accompanied by the Siemens-Westinghouse Company in 1970 [4]. Among the first investigations carried out in this concern [5-8], in 2000 that company set up the first 100 kW fuel cell power plants operating at the pressure of 300 kPa with a 50 kW micro gas turbine, in the national center for fuel cell research at the University of California [4]. Due to high efficiency (about 65%), controllability of power output and heat recovery capability the SOFC-GT hybrid systems have attracted the studies of numerous investigators. The technology of the tubular solid oxide fuel cell was studied by Singhal [9] and after then different thermodynamic and mathematical models of SOFC-GT have been derived and developed by numerous research groups [10-23].

Corresponding Author: M.Y. Abdollahzadeh Jamalabadi, Maritime University of Chabahar, Chabahar, Iran.

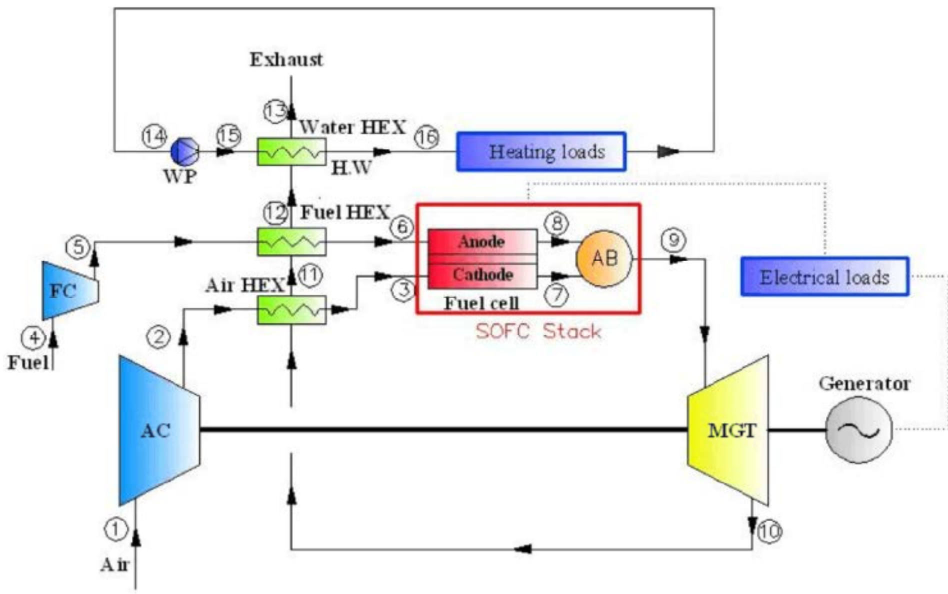

Fig. 1: Schematic of SOFC-MGT system.

The goal of the present research is to economic study a CHP system using of solid oxide fuel cell and mini gas turbine (SOFC-MGT) for concurrent production of electrical and thermal energies with high efficiency with respect to the environmental concerns. Initially a hybrid system along with its supplementary equipment has been simulated and then, every noted cycle component has been thermodynamically analyzed with a complete electrochemical and thermal analysis has also been performed for the fuel cell used for the system. Then over and done with a parametric study of the mentioned hybrid system, the effects of the rate of air and fuel flows into the system, working pressure ratio, fuel cell current density, fuel unit cost, electricity price,and capital cost, on the efficiency, power production, total cost rate and the rate of exergy destruction have been examined to find the optimum electrical energy cost and payback period of the investment.

Hybrid System Configuration: The representation of the studied hybrid SOFC-GT system has been revealed in Fig. 1. The suggested system consists of a stack of solid oxide fuel cell with internal reforming, afterburner chamber, mini turbine, air compressor, fuel compressor, water pump and three recuperators. All thermal processes of that SOFC-MGT hybrid system in a simplified manner and is close to the first real constructed system of its kind. The energies used in a building include the heating, cooling and the electrical loads and the offered SOFC-MGT system must be talented to deliver them. The composition of the used air (point 1) is assumed to include 21% oxygen and 79% nitrogen and the utilized fuel (point 4) in the system is natural gas with the composition of 97% methane, 1.5% carbon dioxide and 1.5% nitrogen.

Assumptions: In the steady modeling and analysis of the proposed system, the gas leakage from the system and the change in kinetic and potential energy, the change in temperature and pressure inside the cell, are disregarded. Also the gas modeled as an ideal gas and USUF thermodynamic assumption is considered for the gasses exiting the cathode and anode. As well the fuel inside the fuel cell is assumed to process into hydrogen via internal reforming.

The Governing Equations: In this section, the equations used for modeling the SOFC-MGT different sections are presented. For thermal modeling of the system in steady state condition the average values of the thermodynamic parameters at each component were applied and for thermophysical properties of gases, a temperature dependent specific heat model based on empirical polynomials for ideal gas was applied.

Fuel Cell: The model for the proposed SOFC-MGT system is provided in three separate sections of reforming, electrochemical and thermal calculations as:

Reforming Calculations: At the anode of a SOFC the water production reaction ($H_2 + O^{-2} \rightarrow H_2O + 2e^-$) and at its cathode the oxygen consumption reaction ($\frac{1}{2}O_2 + 2e^- \rightarrow O^{-2}$) exist. Before this reactions the methane gas must be converted to hydrogen in reforming and shifting reactions. A SOFC can use of hydrogen and carbon monoxide as fuel. The fact that through direct internal reforming, carbon monoxide and methane can be used as fuel inside the fuel cell is very important. The reactions that take place in the internal reforming process are highly endothermic and get their needed heat from the fuel cell. The use of this method reduces, to some extent, the dependence of the cell on a cooling system. The reactions carried out in this process are [13,24]:

$$x \rightarrow [CH_4 + H_2O \leftrightarrow CO + 3H_2] \text{ (Reforming)} \tag{1}$$

$$y \rightarrow [CO + H_2O \leftrightarrow CO_2 + H_2] \text{ (Shifting)} \tag{2}$$

$$z \rightarrow [H_2 + 1/2O_2 \leftrightarrow H_2O] \text{ (Overall cell reaction)} \tag{3}$$

Relations (1) and (2) represent the steam reforming and the water and gas shifting reactions, respectively. Based on the reforming reactions, the natural gas (CH_4) is converted into hydrogen inside the fuel cell and then, this hydrogen participates in the cell electrochemical reaction, according to relation (3) [25]. In the above relations, *x, y* and *z* represent the molar rates of progress of the cell reforming, shifting and overall reactions, respectively. By balancing the masses of various gasses in equilibrium, the molar rates of outflow gasses from the cell will be determined according to the following:

$$\begin{aligned}
[\dot{n}_{CH4}]^{out} &= [\dot{n}_{CH4}]^{in} - x \\
[\dot{n}_{H2O}]^{out} &= [\dot{n}_{H2O}]^{in} - x - y + z \\
[\dot{n}_{H2}]^{out} &= [\dot{n}_{H2}]^{in} + 3x + y - z \\
[\dot{n}_{CO}]^{out} &= [\dot{n}_{CO}]^{in} + x - y \\
[\dot{n}_{CO2}]^{out} &= [\dot{n}_{CO2}]^{in} + y \\
[\dot{n}_{tot}]^{out} &= [\dot{n}_{tot}]^{in} + 2x
\end{aligned} \tag{4}$$

Considering the above equations, the partial pressures of gasses exiting the anode and cathode will be obtained as:

$$P_i = \frac{\dot{n}_i}{\dot{n}_{tot}} \cdot P_{tot} \tag{5}$$

The reforming and shifting reactions are equilibrium reactions [26]. The relation between the amounts of components that are in equilibrium, composition of the equilibrium and its final temperature is established by the equilibrium constants. For the two reactions of reforming and shifting, equilibrium constants are defined as:

$$Kp,r = \frac{P_{H2}^3 \cdot P_{CO}}{P_{CH4} \cdot P_{H2O}} \tag{6}$$

$$Kp,sh = \frac{P_{CO2} \cdot P_{H2}}{P_{CO} \cdot P_{H2O}} \tag{7}$$

Considering relations (4) to (7) and also taking into account the electrochemical reaction of the cell, the following relations will be obtained:

$$Kp,r = \frac{\left([\dot{n}_{H2}]^{in} + 3x + y - z\right)^3 \cdot \left([\dot{n}_{CO}]^{in} + x - y\right)}{\left([\dot{n}_{CH4}]^{in} - x\right) \cdot \left([\dot{n}_{H2O}]^{in} - x - y + z\right)} \cdot \frac{P_{cell}^2}{\left([\dot{n}_{tot}]^{in} + 2x\right)^2} \tag{8}$$

$$Kp,sh = \frac{\left([\dot{n}_{CO2}]^{in} + y\right) \cdot \left([\dot{n}_{H2}]^{in} + 3x + y - z\right)}{\left([\dot{n}_{CO}]^{in} + x - y\right) \cdot \left([\dot{n}_{H2O}]^{in} - x - y + z\right)} \tag{9}$$

$$U_f = \frac{z}{3x + y} \rightarrow z = U_f \cdot (3x + y) \tag{10}$$

In relation (10), U_f is the fuel utilization coefficient, defined as the ratio of the reacted hydrogen in the anode to the input hydrogen into the anode (this value in this paper is assumed as 0.8). The chemical balance achieve at minimum Gibbs function so equilibrium constant of a chemical reaction can calculated by difference of the standard Gibbs function ($\ln Kp = -\frac{\Delta G_0}{R_u T}$). Considering the above relations, the equilibrium constant for a mixture of ideal gasses is only a function of temperature [13]:

$$Log\, Kp = AT^4 + BT^3 + CT^2 + DT + E \tag{11}$$

In the above relation, *A*, *B*, *C*, *D* and *E* are empirical constants [13]. As the first step of this research, the systems of nonlinear governing equations (equations 8-10) are solved and the quantity and composition of the outflow gasses from the fuel cell are determined.

Electrochemical Calculations: The reversible voltage of the fuel cell is given by the Nernst equation [27] as:

$$E = E^{\circ} + \frac{R_u T}{n_e F} \cdot \ln\left(\frac{P_{H_2} \cdot P_{O_2}^{1/2}}{P_{H_2O}}\right) \quad (12)$$

where $E^{\circ} = -\frac{\Delta G_0^{\circ}}{n_e F}$ is the fuel cell voltage at standard conditions (298 Kelvin degree of temperature and 1 bar pressure), R_u is Gas constant, T is Stack cell temperature, F is faraday constant, ΔG_0° is the value of standard Gibbs function for the reaction and n_e is the number of electrons produced in reaction ($n_e = 2$). To calculate the real voltage of the cell, the losses associated with the cell (cell over potential), which includes the activation loss (V_{act}), ohmic loss (V_{ohm}) and the concentration loss (V_{conc}) are computed. Then, the magnitude of the real voltage of the fuel cell (V_{cell}) is obtained through the following relation [28-30]:

$$V_{cell} = E - \left(V_{act} + V_{ohm} + V_{conc}\right) = E - V_{Loss} \quad (13)$$

After calculating the mentioned voltage losses, the real cell voltage will be obtained through equation (13). The activation-related loss consists of the losses associated with the cell startup and also with overcoming all the electrochemical reactions. The magnitude of this loss is equal to the sum of activation over potentials of the cells' anode and cathode and it is found through the simplification of the Butlere-Volmer equation. Also Resistances against electron movements in the anode, cathode and the internal connectors and against ion movements in the electrolyte cause Ohmic voltage losses. On this basis, Ohmic voltage loss or over potential (for anode, cathode, internal connectors and electrolyte). The component of the loss voltages are as follows [31].

$$V_{act} = \frac{2R_u T}{n_e F}\sinh^{-1}\left(\frac{i}{i_0}\right), V_{ohm} = i\delta A' e^{B'/T}$$
$$V_{conc} = \frac{R_u T}{n_e F}\ln\left(1 - \frac{j}{j_L}\right) \quad (14)$$

where i and i_0 are the current density and the exchange current density, respectively and the values of A_0, B_0 and δ, which are fixed parameters, are determined based on the type of the fuel cell. The values of these parameters have been listed in [31]. The total activation loss is the summation of that value at the cathode ($i_{\circ,an} = \gamma_{an}\left(\frac{p_{H_2}}{p_{ref}}\right)\left(\frac{p_{H_2O}}{p_{ref}}\right)\exp\left(-\frac{E_{act,an}}{R_u T}\right)$) and at anode ($i_{\circ,ca} = \gamma_{ca}\left(\frac{p_{O_2}}{p_{ref}}\right)^{0.25}\exp\left(-\frac{E_{act,ca}}{R_u T}\right)$). The calculation of the exchange current density is very complicated and for the anode and cathode of a SOFC, these values are obtained from the following two semi-empirical relations [31]. Knowing the relationship between the current density and the area of the cell, the amount of current and power of each cell will be determined as:

$$I_{cell} = iA_{cell} \quad (14)$$
$$Power_{DC-cell} = V_{cell} I_{cell} \quad (15)$$

Having determined the amount of current and power in each cell, the total current and power outputs of the cell stack can be specified using:

$$I_{tot} = 2Fz \quad (16)$$

$$Power_{DC-tot} = V_{cell} I_{tot} \quad (17)$$

$$Power_{AC-tot} = Power_{DC-tot} \cdot \eta_{inv,cell} \quad (18)$$

$$n = Power_{DC-tot} / Power_{DC-cell} \quad (19)$$

Where η_{inv} is the coefficient of inversion of direct to alternating current.

Thermal Calculations: The temperature of outflow gasses from the fuel cell can be calculated by balancing the energy and also through the use of the iterative method. Since the reforming reactions are endothermic and the shifting and electrochemical reactions are exothermic, the total net heat transfer of the SOFC is determined from the thermal value differences of the three cited reactions, according to the following relation [31]:

$$\dot{Q}_{net} = \dot{Q}_{elec} + \dot{Q}_{sh} - \dot{Q}_r \quad (20)$$

The thermal value of the three cited reactions is determined as:

$$\dot{Q}_r = \dot{x}\left(\bar{h}_{CO} + 3\bar{h}_{H2} - \bar{h}_{CH4} - \bar{h}_{H2O}\right) \quad (21)$$

$$\dot{Q}_{sh} = \dot{y}\left(\bar{h}_{CO2} + \bar{h}_{H2} - \bar{h}_{CO} - \bar{h}_{H2O}\right) \quad (22)$$

$$\dot{Q}_{elec} = \dot{z} \cdot T \cdot \Delta S - I \cdot \Delta V_{Loss}$$
$$\Delta S = \left(S_{H2O}^{\circ} - S_{H2}^{\circ} - \frac{1}{2}S_{O2}^{\circ}\right) + \frac{R_u}{2} \cdot \ln\left(\frac{p_{H2}^2 \cdot p_{O2}}{p_{H2O}^2}\right) \quad (23)$$

A portion of this leftover net heat is spent on raising the temperature of the gasses inside the cell and the gasses exiting the cell $(\dot{Q}')$ and another portion enters the surrounding environment $(\dot{Q}_{surr})$; hence:

$$\dot{Q}_{net} = \dot{Q}' + \dot{Q}_{surr} \quad (24)$$

In the real situation, none of the processes inside the fuel cell can be considered adiabatic and there is always some heat loss into the surrounding. By considering the problem in an ideal state, it is assumed that the fuel cell is adiabatic and that the leftover net heat is spent on raising the temperature of the gasses inside and gasses exiting the fuel cell $(\dot{Q}')$. In this case, by considering identical temperatures for the gasses exiting the anode and cathode, relation ($(n_{ca}\bar{h}_{ca} + n_{an}\bar{h}_{an})_{out} - (n_{ca}\bar{h}_{ca} + n_{an}\bar{h}_{an})_{in}$) will be obtained:

$$\dot{Q}'' = \Delta h_{ca,in} + \Delta h_{ca,out} + \Delta h_{an,in} + \Delta h_{an,out} \quad (25)$$

In this relation, $\Delta h_{ca,in}$ and $\Delta h_{ca,in}$ are the enthalpy changes of reacting agents in the anode and cathode and $\Delta h_{ca,out}$ and $\Delta h_{an,out}$ are the enthalpy changes of resulting products in the anode and cathode. The mentioned values are obtained according to relations (26) and (27).

$$\Delta h = \int_{Tin}^{Tout} c_p dT \quad (26)$$

$$\dot{Q}' = n_3\int_{T_3}^{T_{out}} c_p dT + n_6\int_{T_6}^{T_{out}} c_p dT + n_7\int_{T_3}^{T_{out}} c_p dT + n_8\int_{T_6}^{T_{out}} c_p dT \quad (27)$$

In relation (27), n_3, n_6, n_7 and n_8 are the molar flows of gasses at the inlet and outlet of the cell and c_p is their heat capacity, as a function of temperature. To calculate the temperature of gasses exiting the fuel cell, an iterative algorithm has been used in which the convergence criterion has been considered as relation (28).

$$Q_{error} = \left|\frac{\dot{Q}'' - \dot{Q}'}{\dot{Q}'}\right| < 0.01 \quad (28)$$

After estimating the output temperature, the thermal losses in the fuel cell can be calculated by using the energy relation:

$$\left(\dot{n}_3\bar{h}_3 + \dot{n}_6\bar{h}_6\right) = \dot{Q}_{surr} + \dot{W}_{sofc} + \left(\dot{n}_7\bar{h}_7 + \dot{n}_8\bar{h}_8\right) \quad (29)$$

The values of entropy production and exergy destruction rate will also be obtained by means of the following relations:

$$\dot{S}_{gen,sofc} = \left(\dot{n}_7\bar{s}_7 + \dot{n}_8\bar{s}_8\right) - \left(\dot{n}_3\bar{s}_3 + \dot{n}_6\bar{s}_6\right) + \frac{\dot{Q}_{surr}}{T_{surr}} \quad (30)$$

$$\dot{E}_{D,sofc} = \dot{E}_3 + \dot{E}_6 - \dot{E}_7 - \dot{E}_8 - \dot{E}_Q - \dot{W}_{sofc} \quad (31)$$

Air and Fuel Compressor: Assuming an adiabatic compression, the compressor work is determined by [18]:

$$\frac{T_{2s}}{T_1} = \left(\frac{P_2}{P_1}\right)^{\frac{k_a-1}{k_a}} = \left(r_{p,a}\right)^{\frac{k_a-1}{k_a}} \quad (32)$$

$$\eta_{is,c} = \frac{w_{c,s}}{w_c} = \frac{h_{2s} - h_1}{h_2 - h_1} = \frac{T_{2s} - T_1}{T_2 - T_1} \quad (33)$$

$$\dot{W}_c = \dot{n}_a\left(\bar{h}_2 - \bar{h}_1\right) \quad (34)$$

Also, generated entropy and the exergy destruction rate during the compression process can be obtained through the following relations:

$$\dot{S}_{gen,c} = \dot{n}_a\left(\bar{s}_2 - \bar{s}_1\right) \quad (35)$$

$$\dot{E}_{D,c} = \dot{W}_c - \dot{n}_a\left(e_2 - e_1\right) \quad (36)$$

The calculations performed for the fuel compressor are similar to those for the air compressor. It is necessary to point out that in the present research, the temperatures of the air and fuel entering the system have been assumed as identical.

Afterburner: Taking the chamber efficiency into consideration, the temperatures of the out flowing gasses are calculated based on this equation:

$$\dot{n}_7\bar{h}_7 + \dot{n}_8\bar{h}_8 - \dot{n}_9\bar{h}_9 - \dot{Q}_{loss,ab} = 0 \quad (37)$$

where $\dot{Q}_{Loss,ab}$ is the heat loss of the afterburner chamber and its value depends on the chamber efficiency (η_{ab}), fuel utilization coefficient in the fuel cell (U_f) and the heat value of the fuel (*LHV*) as [18]:

$$\dot{Q}_{Loss,ab} = \dot{n}_4 \cdot \left(1 - U_f\right) \cdot \left(1 - \eta_{ab}\right) \cdot LHV \quad (38)$$

$$\eta_{ab} = \frac{f_{theoretical}}{f_{actual}} \quad (39)$$

The amount of entropy generation and exergy destruction rate in this chamber is found from:

$$\dot{S}_{gen,ab} = \dot{n}_9\bar{s}_9 - \dot{n}_7\bar{s}_7 - \dot{n}_8\bar{s}_8 + \frac{\dot{Q}_{loss,ab}}{T_{surr}} \quad (40)$$

$$\dot{E}_{ab} = \dot{E}_7 + \dot{E}_8 - \dot{E}_9 - \dot{E}_{Q,ab} \quad (41)$$

Mini Turbine: The hot gasses that leave the afterburner chamber then enter the turbine and generate electric current. By calculating ideal work and considering the isentropic efficiency of the turbine, the amount of work and output temperature of the turbine can be determined:

$$\eta_{is,mgt} = \frac{W_{mgt,a}}{W_{mgt,s}} = \frac{\bar{h}_9 - \bar{h}_{10}}{\bar{h}_9 - \bar{h}_{10s}} = \frac{T_9 - T_{10}}{T_9 - T_{10s}} \quad (42)$$

The following relations can be used to determine the temperature of air leaving the turbine and the amount of work produced by the turbine:

$$P_{10} = P_9 \left(\frac{T_{10S}}{T_9} \right)^{\frac{k_g}{k_g - 1}} \quad (43)$$

$$\dot{W}_{mgt} = \dot{n}_9 \left(\bar{h}_9 - \bar{h}_{10} \right) \quad (44)$$

The rates of entropy generation and exergy destruction during the expansion process inside the turbine are obtained from the following relations:

$$\dot{S}_{gen,mgt} = \dot{n}_9 \left(\bar{s}_{10} - \bar{s}_9 \right) \quad (45)$$

$$\dot{E}_{D,mgt} = \dot{n}_9 \left(e_9 - e_{10} \right) - \dot{W}_{mgt} \quad (46)$$

Recuperators: In this research, to raise the temperature of the air and fuel entering the cell and also to provide the needed warm water, three external recuperators have been used which are fed by the hot outflow gasses of the turbine. As it was mentioned, a portion of the thermal energy contained in the outflow gasses is used to warm the air and fuel that enter the cell and another portion of this energy enters another recuperator, in order to provide the required thermal load. The gasses temperature leaving the first and the second recuperator is calculated by using:

$$\varepsilon_{reg,1} = \frac{T_4 - T_2}{T_7 - T_2} \quad (47)$$

$$\varepsilon_{reg,2} = \frac{T_5 - T_3}{T_8 - T_3} \quad (48)$$

Also, the following relations are used to estimate the useful thermal load in the third recuperator, based on the efficiency of this recuperator:

$$Q_{reg,3} = \varepsilon_{reg,3} \dot{n}_{12} \left(\bar{h}_{12} - \bar{h}_{13} \right) \quad (49)$$

$$Q_{reg,3} = \dot{n}_w \bar{C}_p \left(T_{16} - T_{15} \right) \quad (50)$$

By using relation (50), the amount of warm water needed for heating systems can be determined. The rates of entropy generation and exergy destruction in the first recuperator are obtained through the following relations:

$$\dot{S}_{gen,reg,1} = \dot{n}_2 \left(\bar{s}_3 - \bar{s}_2 \right) - \dot{n}_{10} \left(\bar{s}_{10} - \bar{s}_{11} \right) \quad (51)$$

$$\dot{E}_{D,reg,1} = \dot{n}_{10} \left(e_{10} - e_{11} \right) - \dot{n}_2 \left(e_3 - e_2 \right) \quad (52)$$

Similar relations have also been used for the other recuperators.

Pump: The work required by the pump is obtained as:

$$\dot{W}_{wp} = \dot{n}_w v_{14} \left(P_{15} - P_{14} \right) \quad (53)$$

Also the entropy generation and exergy destruction rates and the exergy efficiency in the pump are obtained by the following relations:

$$\dot{S}_{gen,wp} = \dot{n}_w \left(\bar{s}_{15} - \bar{s}_{14} \right) \quad (54)$$

$$\dot{E}_{D,wp} = \dot{W}_{wp} - \dot{n}_w \left(e_{15} - e_{14} \right) \quad (55)$$

Hybrid System (SOFC-MGT): The electrical, exergy and overall efficiencies of the hybrid SOFC-MGT system are obtained as follows, respectively:

$$\eta_{ele} = \frac{\dot{W}_{net}}{\dot{n}_f \cdot LHV} \quad (56)$$

$$\psi_{sys} = \frac{\dot{W}_{net} + \dot{E}_{16}}{\dot{E}_1 + \dot{E}_4 + \dot{E}_{14}} \quad (57)$$

$$\eta_{tot} = \frac{\dot{W}_{net} + \dot{Q}_{reg,3}}{\dot{n}_f \cdot LHV} \quad (58)$$

In the above relations, the amount of net power output of the system is equal to the sum of net power outputs of the fuel cell and turbine and also the amount of energy input to the system is equal to the energy released as a result of fuel utilization in the cell and afterburner chamber:

$$\dot{W}_{net} = \left(Power_{AC-tot}\right)_{sofc} + \left(\dot{W}_{AC-net}\right)_{mgt} \tag{59}$$

$$\left(\dot{W}_{AC-net}\right)_{mgt} = \left(\dot{W}_{DC-net}\right)_{mgt} \cdot \eta_{inv,gen} - \dot{W}_{wp} - \dot{W}_{c} - \dot{W}_{cf} \tag{60}$$

$$\left(\dot{W}_{DC-net}\right)_{mgt} = \dot{W}_{mgt} \tag{61}$$

In relation (60), $\eta_{inv,gen}$ is the coefficient of inversion of direct current to alternating current in the turbine generator. The entropy generation, exergy destruction, exergy loss and the irreversibility in the whole system will be obtained by the following relations:

$$S_{gen}^{cyc} = \sum_{i} S_{gen,i} \tag{62}$$

$$\dot{E}_{D,sys} = \dot{E}_1 + \dot{E}_4 + \dot{E}_{14} - \dot{E}_{13} - \dot{W}_{net} - \dot{E}_{16} \tag{63}$$

$$\dot{E}_{L,sys} = \dot{E}_{13} \tag{64}$$

$$\dot{I}_{tot} = \dot{E}_{D,sys} + \dot{E}_{L,sys} \tag{65}$$

Economic and Environmental Analysis: The presented economic analysis make allowance for the capital and repair costs of system components and the operational cost (containing the cost of electricity consumption). Several methods were proposed for the thermo-economic calculation of energy systems such as total revenue requirements and direct method. The goal parameters of the economic modeling is the electricity cost ($ per kilowatt hour) of produced power which is a function of the initial investment cost to purchase the equipment, maintenance costs and fuel costs. In the current analysis the cannibalized income of the equipment in payback calculations are ignored. The investment cost functions are listed in Table 1 [33, 34] for major components in terms of their design parameters.

Unfortunately the prices of the references are for 1994 and are not updated. The cost coefficients of the reference [34] are updated based on the 5 percent annual interest rate from the time of estimation of that prices till now. In order to convert these costs into cost rates per unit time, the following relation is used [34].

$$\dot{C}_K = \left(\frac{C_K \varphi}{3600N}\right)\left(\frac{i(1+i)^n}{(1+i)^n - 1}\right) \tag{66}$$

where the C_K shows the capital cost of K $_{th}$component is estimated based on the cost functions which are listed in Table 1, the second bracket is the is the Capital Recovery Factor (CRF) which is a function of system lifetime (n) in the year units and the annual interest rate (i), ö shows the maintenance factor (1.08) and N is the total working hours of the system per year (here the 80 percent of total time is assumed). Moreover, the operational cost of the whole system including the cost of electricity consumption can be determined as follows:

Table 1: Cost functions for the major components of the SOFC-MGT system

Parameter	Value
Component	Cost function ($)
Compressor (centrifugal)	$91562(P_c/445)^{0.67}$
Gas turbine (radial)	$(-98.328\ln(P_{GT}) + 1318.5)P_{GT}$
Recuperatior	$111.6(m_{HE})^{0.95}$
SOFC stack	$A_{tot,stack}(2.96T_{cell} - 1907)$
Inverter	$100000(P_{cell}/500)^{0.7}$
Generator	$60(P_{GT} - P_c)^{0.95}$
Auxiliary equipment	$0.1\ A_{tot,stack}(2.96T_{cell} - 1907)$
Heat recovery exchanger	$8500 + 405A_t^{0.85}$
pump	271.54m'+1094.7
After burner	$(46.08\ m')(1+\exp(0.018T-26.4))/(\ 0.995-P_r)$

$$c_{elec} = \frac{\dot{W}_{net}}{3600} \tag{67}$$

The Payback period is defined as the time period necessary for the net income received from selling the output of a system (i.e. Electricity and recovered heat) after deductions to get well the initial investment prices of the particular system [34]. Regarding the time value of money, the worth of hybrid system capital investment as well as the fuel consumption costs in the pth year of running can be estimated from the following equation:

$$C_{invest,p} = C_{capital,m} \sum_{m=0}^{p-1} (1+i)^{p-m} + 3600N\dot{C}_{fuel} \sum_{m=1}^{p} (1+i)^{p-m} \tag{68}$$

where i is the annual interest rate and N is the number of running hours per year.

Using SOFC systems incorporating GT imposes additional expenses for investment and operational costs in comparison with that of conventional systems. These extra expenses arise from the capital and maintenance costs of the SOFC as well as the GT. The additional costs can be considered over time with reduction in electricity efficiency of the fuel cell (in comparison with that of conventional systems). But in this research the payback period is calculated by ignoring these additional.

Global warming as the one of the environmental threats on humankinds is considered in the current investigation. The depletion of fossil fuels for electricity generation can made a great amount of CO_2 which is harmful for ozone layer. So the environmental influence is one of the concerns in the analysis of energy systems which is studied in the present study through the hybrid SOFC-MGT system. Other than increase in thermal efficiency of the system the amount of the CO_2 and other emission products should be minimized. As mentioned in the literature search the SOFC-GT power plant produces lowers fuel consumption and then the lower pollutant emissions. Also because of sensitivity of fuel cell parts the inlet fuel should be more purified than the common power plants. In this research, a fine cost was related to the rate of CO_2 emission was added to the system total cost. The penalty cost of CO_2 emission is considered as 0.1 US dollars per kilograms. So the rate of penalty cost of CO_2 emission is:

$$\dot{C}_{env} = \frac{m_{CO_2} C_{CO_2}}{3.6\times10^6 N} \tag{69}$$

Fuel Shipping Costs: A great difference of using SOFC in ship with other application is that in ship costumer should carry the fuel for power generation. For the fuel cost, here the LNG prices are used. Liquefied natural gas (LNG) is natural gas (predominantly methane, CH4) that has been converted to liquid form for ease of storage or transport. Although, it takes up about 1/600th the volume of natural gas in the gaseous state a place for storing the fuel in the ship also should be considered. Nowadays LNG is transported in specially designed ships with double hulls protecting the cargo systems from damage or leaks and a part of that fuel can be used for internal consumption of such ships (The tankers cost around USD 200 million each). LNG shipping costs are a key driver of the value that can be generated from moving gas between different locations, chartering fee, brokerage (1-2% fee), fuel consumption, port costs, canal costs, insurance costs. Here the assumptions are 137,000 m^3 capacity, 10 days average voyage period and 7 average voyages with full cargo per year.

Numerical Solution: The prepared computer program is based on lumped method. This program receives the mass and fuel flow rate as well as the compressor pressure ratio as the input data. Then, the equations are solved and examined by varying the effective parameters. First the nonlinear equations of the reforming and electrochemical processes and the thermal equations of the cell are simultaneously solved and the desired results including the calculations of the composition of output chemicals, temperature, voltage, power, efficiency and the other fuel cell properties are obtained. Then the final calculations of the hybrid system are carried out to the fulfillment of convergence conditions and the efficiency, power production and the rates of entropy generation and exergy destruction of the whole hybrid system are determined. The detailed of the code and its validation against [9], [13] is presented in the [36,37].

RESULTS

The goal of this research is to investigate the impact of the flow rates of air and fuel entering the system and also the effect of working pressure ratio of compressor on the economic and environmentl of the system. The fuel cell used in this research is of the tubular solid oxide type (similar to the model by Siemens-Westinghouse Co.) and the specifications of this cell along with the assumed parameters in the analysis of this hybrid system have been presented in Table 2 [32].

Since the fuel cell is the main source of power generation in the hybrid systems, to obtain more accurate results in this research, comprehensive electrochemical and thermal calculations of the fuel cell were carried out. In spite of the most of the previous research works, the working temperature of the cell has not been presumed as constant and it is a function of the cited parameters.

Effects of Compressor Pressure Ratio : The outflow heat of the SOFC is used in GT in current configuration. So when the compressor pressure ratio increases the relative pressures of gas components increase and due to that the Nernst potential increases. This effect generally causes the more electricity production and so the total price of it decreases as shown in the Figure 2. At low compressor ratio the increase of pressure leads to decrease of the temperature of the cell stack and of the gasses leaving the cell decreases as well. So the lower enthalpy delivered to the GT and the net electricity power generation decreases.

Since the excess of oxygen increase improve the kinetics of chemical reactions and net output power of the SOFC. As can be seen in Figure 5, the reduction of air-to-fuel ratios increases the total cost rates. The maximum prices was achieved at A/F of 10.5 and 12.5.

In Fig. 3, the environmental penalty costs of the hybrid system at different working pressures have been shown. As can be observed, the system environmental penalty costs not only depend on the working pressure, but also on the ratio of air to fuel entering the system.

Table 2: Simulation input parameters [18,32]

Parameter	Value
Cell area (m^2)	0.1
Fuel compressor efficiency (%)	80
Air compressor efficiency (%)	80
Pressure loss in recuperator (%)	5
Pressure loss in fuel cell stack (%)	5
Pressure loss in after burner (%)	5
Inverter efficiency (%)	89
Gas/air recuperator effectiveness (%)	85
Gas/fuel recuperator effectiveness (%)	85
Gas/water recuperator effectiveness (%)	85
Pump efficiency (%)	85
Afterburner efficiency (%)	95
Mini turbine efficiency (%)	84
Generator efficiency (%)	95

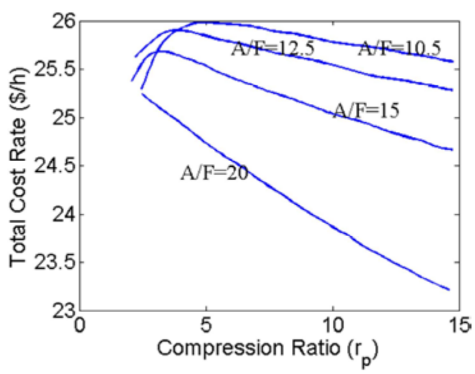

Fig. 2: Variations of total cost rate with system compression ratio for different air to fuel ratios

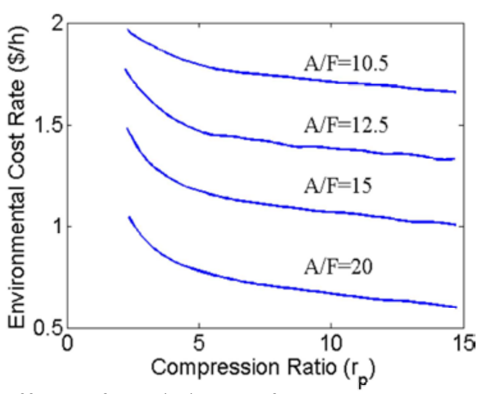

Fig. 3: Effect of variations of system compression ratio and air to fuel ratios on the environmental costs

Contrary to most researches that have presented their results at a constant air-to-fuel ratio, these diagrams indicate that at high air-to-fuel ratios, with the increase of the system pressure ratio, due to the reduction of temperature, the environmental penalty costs decrease. By increase of the pressure ratio, due to having too much

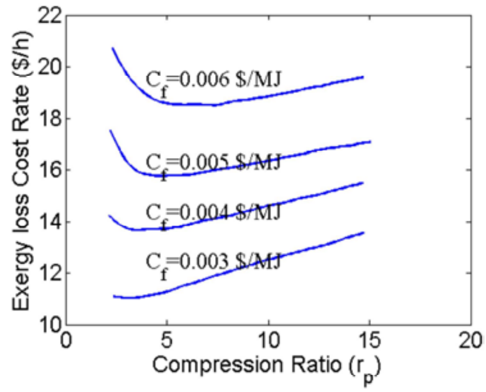

Fig. 4: Effect of system compression ratio on exergy loss cost rate for different air to fuel ratios

fuel and consequently a high temperature, the efficiency of the chemical reforming increases and the pollution of the reactions decreases.

In spite of the most researches the exergy loss through the SOFC-GT is presented here. Regardless of the high efficiency of the SOFC-GT the significant exergy lost still exist in the hybrid system. Figure 4 shows the effect of system compression ratio on exergy loss cost rate for different air to fuel ratios

According to Fig. 4 this exergy loss mostly increases with the increase of compressor ratio and by increase of fuel cost that price increase.

Effects of Air Flow Rate Entering the System : Air flow rate is an important parameter which affects the performance of the cycle; and it is necessary to adjust it at an optimum value to get satisfactory cycle competence. The required air flow rate for the hybrid cycle is determined by the rate of electrochemical reaction, cell temperature and the reactions of the combustion chamber. The volume of arrival air should be sufficient for the oxidation of hydrogen in the cell and of the excess gasses in the afterburner chamber and as well for the cooling of the fuel cell. Alternatively, the excessive increase of the flow rate of air incoming the system will affect the decline of cell temperature (because of its cooling effect) and so, the increase of voltage cost and decrease of efficiency in the hybrid structure. In the accomplished analyses, the flow rate of fuel entering the system has been assumed as 10 (kmol/h). As it is observed in Figure 5, the increase of the flow rate of air passing through the system causes the temperature and thus, the production voltage of the cell to diminution at different working pressures. On the other hand, with the further reduction of the inlet air flow rate, the operational temperature of the cell growths beyond

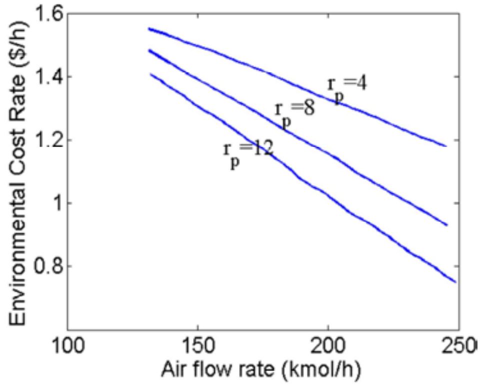

Fig. 5: Variations of environmental costs of the system as a function of compression ratio and air flow rate

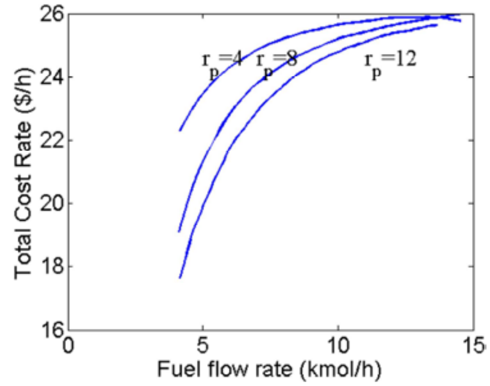

Fig. 6: Variations of total costs of the system as a function of compression ratio and fuel flow rate

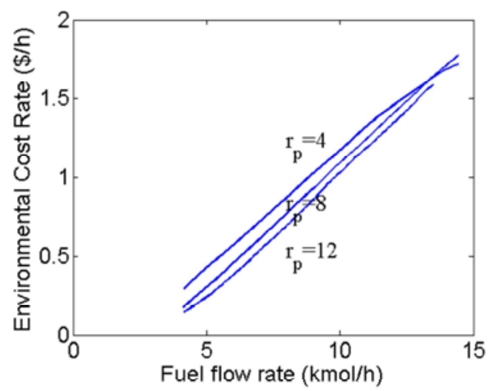

Fig. 7: Environmental costs vs compression ratio and fuel flow rate

the allowed limit (1000°C); and this will damage the cell. As can be seen in Figure 5, the increase of the passing air flow rate will also cause the reduction of emission of the system and its cost.

It is shown in Figure 5 that at a definite functioning pressure, the increase of air flow rate will cause the pollution produced in the hybrid system to decrease. This is despite the fact that the increase of air flow rate always leads to the growth of power making in the turbine; but in the meantime a greater portion of the pollution produced in the hybrid system is delivered by the fuel cell, this increase is not effective enough and the overall pollution of the system diminishes. From the Equation (69) decrease of the CO_2 production decreases the environmental costs.

Effects of Fuel Flow Rate Entering the System: In order to study the influence of fuel flow rate entering the system, this rate is changed while keeping the pressure ratios of air and fuel compressors and the flow rate of incoming air (150 kmol/h) constant. An increasing rate of fuel flow into the system, causes more complete chemical reaction and more energy is being altered into electrical energy in the cell. Thus, more fuel and consequently, more air will be consumed in the cell. An increase of fuel flow rate accompanies an increase of current generation in the fuel cell; the increase of current generation in the cell has a linear correlation with the utilization of hydrogen in the cell. This increase of current leads to the generation of more heat in every single cell of the fuel cell stack, thereby raising the total cost rate until the maximum reasonable reached. With the increase of fuel flow rate, the current density in the cell increases and as a result, the produced electric power will increase. As a whole, the increase of fuel flow rate at a constant fuel utilization coefficient will have a superior impression on excess voltage and on the reduction of voltage generated by the cell after the maximum point in the Figure 6. As can be seen in Fig. 6, the increase of the flow rate of fuel passing through the system at different cell working pressures, also causes the total price of product to raise. Figure 7 shows the environmental costs vs compression ratio and fuel flow rate. As shown by increase of fuel flow rate and decrease of pressure ration, the CO_2 production rate increases dramatically (And so it's cost from the equation 69). Increasing the fuel flow rate at constant fuel utilization coefficient, increase the reaction rate of the cell and in the long run lead to the increase of pollutant production in the fuel cell of the hybrid system. A sensitivity analysis of the exergy loss cost in the system respect to the fuel cost is done in the Figure 8. As presented by increase of fuel flow rate and decrease of pressure ration, the penalty of the exergy loss through the system increases vividly.

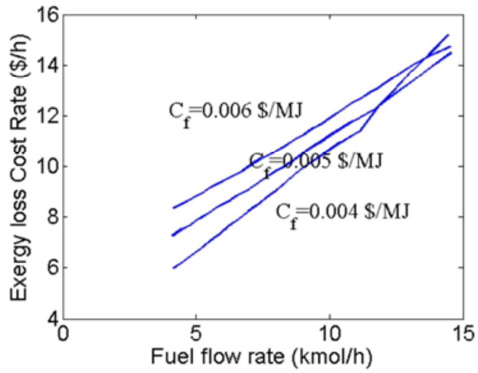

Fig. 8: Effect of fuel flow rate on electrical efficiency for different cell pressures

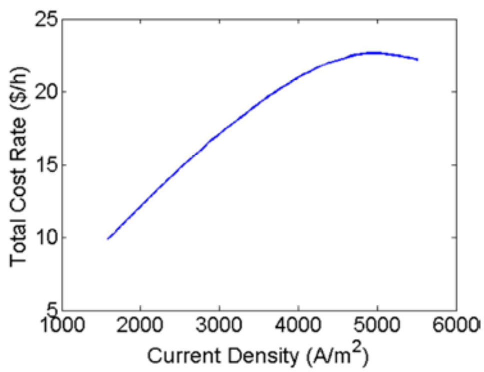

Fig. 9: Variations of exergy destruction rate with fuel flow rate for different cell pressures

Effects of Cell Current: The increase of fuel cell electric current the power production rate increases. However, to reach that the more chemical reactions and so the more input fuel is required. Increasing the cost of fuel at constant fuel utilization coefficient, will compensated by the increase of the electric power of the cell at the 5000 A/m^2. This fact is shown at the Figure 8. As presented the maximum change of the total cost rate occurs by the change of current density rather than other parameters.

Electrical Energy Cost and Payback Period: Finally, according to Eq. (68), the payback period of extra cost for the hybrid system, relative to a conventional system, is estimated 5.4 years and the electrical energy cost is obtained 0.09 $\$kW^{-1}h^{-1}$, while this value is estimated 8.4 years and 1.5 $\$kW^{-1}h^{-1}$when simple SOFC system is used. Even though the extra costs of the hybrid system is over and above that of simple SOFC and conventional systems, these additional expenses possibly will be recompensed in less than five years due to increase in heat production in heat exchangers and electricity

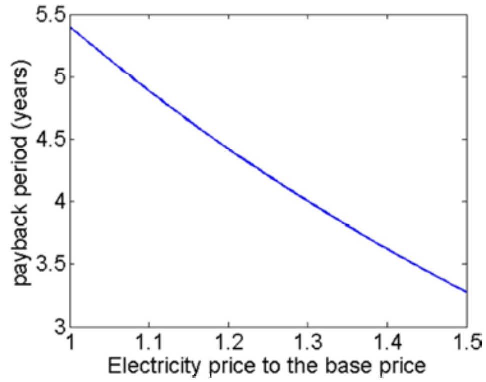

Fig. 10: Variations of the payback period to the electricity price

production in GT. Therefore, utilizing the hybrid system is strongly recommended for electricity production applications owing to its lower fuel consumption and also lower CO_2 emission.

By decrease of investment prices, repair and maintenance costs, the fuel price and by increase of the electricity price the payback time decreases. The sensitivity analysis for the variation of the payback period to the electricity price at the constant investment cost but at fuel costs increased by rate of 10 percent per year is presented in the Figure 10. In that case by increase of 50% in the electricity costs the capital cost the payback time is decreased to 3.3 years.

CONCLUSION

In this study, economic and environmental analysis of a CHP system using SOFC-MGT is explored. By performing a complete electrochemical, thermal and exergetic analysis for the hybrid system on the effect of variation of the working pressure , rate of air flow into the system, fuel cell current density, fuel unit cost , capital cost ,and electricity price to assessing the total cost rate including investment, operational and environmental are investigated. Results found that the electrical energy costs and payback period of the investment and utilizing the hybrid system is strongly recommended for electricity production applications owing to its lower fuel consumption and also lower CO_2 emission.

Nomenclature:

A = Area (m^2)
C = Cost ($)
c_p = Specific heat at constant pressure (kJ/kmol K)

e = Specific exergy flow (kW/kg)
E = Reversible voltage of the fuel cell (V)
E^0 = Fuel cell voltage under standard conditions (V)
E_D = Exergy destruction
E_L = Exergy lost
F = Faraday's constant (96485 C/mol)
h = Enthalpy (kJ/kmol)
i = Current density (A/m^2)
I = Current (A)
Kp = equilibrium constant
k = Ratio of specific heats
LHV = Lower heating value (kJ/kmol)
n = Molar flow rate (kmol/s)
n_e = Number of electrons
P = Pressure (kPa)
Q = Heat generation rate (kW)
r_p = Compression ratio
R_u = Universal gas constant (8.314 J/mol.K)
s = Entropy (kJ/kmol K)
T = Temperature (K)
U_f = Fuel utilization coefficient
V_{act} = Activation loss (V)
V_{conc} = Concentration loss (V)
V_{ohm} = Ohmic loss (V)
V_{loss} = Voltage loss (V)
V_{cell} = Cell voltage (V)
W = Power (kW)
x = Molar rates of progress of the cell reforming reactions (kmol/s)
y = Molar rates of progress of the cell shifting reactions (kmol/s)
z = Molar rates of progress of the cell overall reactions (kmol/s)

Greek Letters:

η = Efficiency
v = Specific volume

Subscripts:

a = Air
ab = Afterburner
an = Anode
AC = Alternating currentþ
ca = Cathode
c = Air compressor
cell = Fuel cell
cf = Fuel compressor
DC = Direct current
elec = Overall reactions
ele = Electrical
f = Fuel
i = Gas species
in = Inlet
inv = Inverter
is = Isentropic
g = Gas
mgt = Mini gas turbine
out = Exit
r = Reforming reaction
reg = Recuperator
sofc = Solid oxide fuel cell
sh = Shifting reaction
surr = Surrounding
sys = System
th = Thermal
tot = Overall
w = Water
wp = Water pump

REFERENCES

1. Ho Lee, K. and R.K. Strand, 2009. SOFC cogeneration system for building applications, part 1: Development of SOFC system-level model and the parametric study, J. Renew. Energy. 34: 2831-2838.
2. Paska, J., P. Biczel and M. K1os, 2009. Hybrid power systems - An effective way of utilising primary energy sources, J. Renew. Energy. 34: 2414-2421.
3. Ho Lee, K. and R.K. Strand, 2009. SOFC cogeneration system for building applications, part 2: System configuration and operating condition design, J. Renew. Energy. 34: 2839-2846.
4. Bessette, N.F. and J.F. Pierre, 2000. Status of Siemens Westinghouse tubular solid oxide fuel cell technology and development program, Proceedings of the 2000 Fuel Cell Seminar, Courtesy Associates.
5. Harvey, S.P. and H.J. Richter, 1994. Gas turbine cycles with solid oxide fuel cells, part I and II, J. Energy Resour. Technol., 116: 305-318.
6. Lee, G. and F. Sudhoff, 1996. Fuel cell/gas turbine system performance studies, Fuel Cells '96 review meeting, Morgantown, West Virginia, DOE/METC/C-97/7278.

7. Chaney, J., R. Tharp, W. Wolf, A. Fuller and J. Hartvigson, 1999. Fuel cell/micro turbine combined cycle, Final Report, McDermott Technology, Inc.,
8. Massardo, A.F. and F. Lubelli, 2000. Internal reforming solid oxide fuel cell-gas turbine combined cycles (IRSOFC-GT): part I - cell model and cycle thermodynamic analysis, J. Eng. Gas Turbine., 122: 27-35.
9. Singhal, S.C., 2000. Advances in solid oxide fuel cell technology, J. Solid State. Ion., 135: 305-313.
10. Costamagna, P., L. Magistri and A.F. Massardo, 2001. Design and part-load performance of a hybrid system based on a solid oxide fuel cell reactor and a micro gas turbine, J. Power Sources. 96(2): 352-368.
11. Palsson, J., Thermodynamic modeling and performance of combined solid oxide fuel cell and gas turbine system, Ph.D Thesis, Dept. Heat and Power Engineering, Lund University of Sweden.
12. Selimovic, A., 2002. Modeling of solid oxide fuel cells applied to the analysis of integrated systems with gas turbines, Ph.D Thesis, Dept. Heat and Power Engineering, Lund University of Sweden.
13. Chan, S.H., H.K. Ho and Y. Tian, Modeling of simple hybrid solid oxide fuel cell and gas turbine power plant, J. Power Sources. 109: 111-120.
14. Uechi, H., S. Kimijima and N. Kasagi, Cycle analysis of gas turbine-fuel cell cycle hybrid micro generation system, J. Eng. GasTurbine., 126: 755-762.
15. Rajashekara, K., 2004.Hybrid fuel cell strategies for clean power generation, Conf. Trans. Ind. Appl., 3: 2077-2083.
16. Motahar, S. and A.A. Alemrajabi, 2009. Exergy based performance analysis of a solid oxide fuel cell and steam injected gas turbine hybrid power system, J. Hydrog. Energy. 34: 2396-2407.
17. Lai, W.H., C.A. Hsiao, C.H. Lee, Y.P. Chyou and Y.C. Tsai, 2007. Experimental simulation on the integration of solid oxide fuel cell and micro-turbine generation system, J. Power Sources. 171 : 130-139.
18. Haseli, Y., I. Dincer and G.F. Naterer, 2008. Thermodynamic analysis of a combined gas turbine power system with a solid oxide fuel cell through exergy, J. Thermochim. Acta. 480: 1-9.
19. Cocco, D. and V. Tola, Externally reformed solid oxide fuel cell-micro-gas turbine (SOFC-MGT) hybrid systems fueled by methanol and di-methyl-ether (DME), J. Energy. 34: 2124-2130.
20. Komatsu, Y. and S. Kimijima, Performance analysis for the part-load operation of a solid oxide fuel cell-micro gas turbine hybrid system, J. Energy. 35: 982-988.
21. Zhao, Y., N. Shah and N. Brandon, 2011. Comparison between two optimization strategies for solid oxide fuel cell-gas turbine hybrid cycles, J. Hydrog. Energy. 36: 10235-10246.
22. Zhao, Y., J. Sadhukhan, A. Lanzini, N. Brandon and N. Shah, 2011. Optimal integration strategies for a syngas fuelled SOFC and gas turbine hybrid, J. Power Sources. 196: 9516-9527.
23. Cheddie, D.F., 2011. Thermo-economic optimization of an indirectly coupled solid oxide fuel cell/gas turbine hybrid power plant, J. Hydrog. Energy. 36: 1702-1709.
24. Chan, S.H., K.A. Khor and Z.T. Xia, 2001. A complete polarization model of a solid oxide fuel cell and its sensitivity to the change of cell component thickness, J. Power Sources. 93: 130-140.
25. Williams, M.C., 2004. Fuel Cell Handbook, 7th Ed., U.S Department of Energy, Virginia.
26. Ghanbari P., 2007. Bavarsad, Energy and exergy analysis of internal reforming solid oxide fuel cell-gas turbine hybrid system, J. Hydrog. Energy. 32: 4591-4599.
27. Bo, C., C. Yuan, X. Zhao, C.B. Wu, Li. and M. Qing, Parametric analysis of solid oxide fuel cell, J. Clean. Technol. Environ. Policy. 11(4): 391-399.
28. Akkaya, A.V., B. Sahin and H.H. Erdem, 2007. Exergetic performance coefficient analysis of a simple fuel cell system, J. Hydrog. Energy. 32: 4600-4609.
29. Akkaya, A.V., 2007. Electrochemical model for performance analysis of a tubular SOFC, J. Energy Research, 31: 79-98.
30. Akkaya, A.V., B. Sahin and H.H. Erdem, 2008. An analysis of SOFC/GT CHP system based on exergetic performance criteria, J. Hydrog. Energy. 33: 2566-2577.
31. Akkaya, A.V., 2007. Electrochemical model for performance analysis of a tubularSOFC. Journal of Energy Research, 31: 79-98.
32. Ciesar, J.A., 2001. Hybrid systems development by the Siemens Westinghouse power corporation, Presented in: U.S. department of energy, Natural Gas/Renewable Energy Hybrids Workshop.
33. Calise, F., M. Denticed'Accadia, A. Palombo, L. Vanoli and M.R. Von Spakovsky, 2006. Single-level optimization of a hybrid SOFC-GT power plant, J. Power Sources, 159: 1169-1185.
34. Bejan, A., G. Tsatsaronis and M. Moran, 1996. Thermal Design and Optimization, John Wiley and Sons, New York,

35. Siemens-Westinghouse Power Corporation, Pressurized Solid Oxide Fuel Cell Gas Turbine Power System. Final Report, for US Department of Energy, February 2000.
36. Abdollahzadeh Jamalabadi, M.Y., 2013. Electrochemical and Exergetic Modeling of a Combined Heat and Power System Using Tubular Solid Oxide Fuel Cell and Mini Gas Turbine, J. Fuel Cell Sci. Technol., 10(5): 051007.
37. Abdollahzadeh Jamalabadi, M.Y., J.H. Park and C.Y. Lee, 2014. Economic and environmental modeling of a micro gas turbine and solid oxide fuel cell hybrid combined heat and power system, International Journal of Applied Environmental Sciences, 4(9): 1769-1781.